

# Free-Space Optical Communication for CubeSats in Low Lunar Orbit (LLO)

Peter M. Goorjian\*

NASA Ames Research Center, M. S. 258-1, Moffett Field, CA 94035-1000, USA

## ABSTRACT

A fine pointing capability has been developed for laser beam pointing to augment body pointing by CubeSats. An application is made to CubeSats in Low Lunar Orbit (LLO), at 100 km. Body pointing was used by Aerospace Corporation for CubeSats in LEO in NASA's Optical Communications and Sensors Demonstration (OCSD) program. Computer simulations of this fine pointing capability have been applied to the OCSD program. With fine pointing, the spot size on the Earth could be reduced by a factor of eight with a reduction in laser output power by a factor of sixty-four, thereby mitigating the thermal load challenge on the CubeSats. The same reductions in spot size and laser output power can be achieved for CubeSats in LLO. The new method uses laser arrays for fine laser beam pointing and does not use moving parts. It combines a lens system and a VCSEL/Photodetector Array. For these electro-optical systems, reaction times to pointing changes and vibrations are on a nanosecond time scale, much faster than those for mechanical systems. Results from computer simulations will be presented.

**Keywords:** space, optical, communications, laser, beam, pointing.

\* Peter M. Goorjian: [peter.m.goorjian@nasa.gov](mailto:peter.m.goorjian@nasa.gov)

## 1 INTRODUCTION

The NASA ARTEMIS Program will include the LunaNet, a highly extensible, open architecture lunar communications and navigation network. A constellation of CubeSats in Low Lunar Orbit (LLO), 100 km, could form an optical communications and navigation network as part of LunaNet, with terminals on the lunar surface, including mobile ones such as with astronauts and rovers. The proposed CubeSat nodes should provide data relay and navigational aid services. A fine pointing capability has been developed for laser beam pointing to augment body pointing by CubeSats. In this paper an application is made to CubeSats in Low Lunar Orbit (LLO), at 100 km. Body pointing was used by Aerospace Corporation for the CubeSats in LEO in NASA's Optical Communications and Sensors Demonstration (OCSD) program<sup>1</sup>. Computer simulations of this fine pointing capability have been applied to the OCSD program<sup>2,3</sup>. With fine pointing, the spot size on the Earth could be reduced by a factor of eight with a reduction in laser output power by a factor of sixty-four, thereby mitigating the thermal load challenge on the CubeSats. The same reductions in spot size and laser output power can be achieved for CubeSats in LLO.

This new method uses laser arrays for fine pointing of laser beams and does not use moving parts. It combines a lens system and an array of vertical-cavity, surface-emitting lasers and photodetectors, VCSEL/Photodetector Array, (both mature technologies), in a novel way. This system is applied to augment body pointing by CubeSats in LLO. Also, it may be able to replace current architectures which use dynamical systems<sup>4</sup>, (i.e., moving parts) to fine-point the laser beam, and it may also be used to replace vibration isolation platforms.

Possible additional applications are to planetary distances (deep space optical communications, DSOC), to optical multiple access (OMA), since laser beams from different sources come in at different angles and then get mapped to different photodetectors; as a result, different beams can be sent back to different sources, and to communication among a constellation of close satellites, which is similar to OMA.

Also, this system may be applicable to satellites that use modulating retro-reflectors<sup>5</sup> by increasing the returning beam power. Current planned architectures envision a high-powered laser at the ground terminal and a modulating retro-reflector at the satellite. The retro-reflector can be replaced with a VCSEL array in the satellite for a strong return response to a weak signal laser beam. This replacement allows for the use of low power lasers at the ground terminal. Also, backscatter, often a limiting factor with a retro-reflected beam, is reduced by using a weaker laser beam from the ground and returning a strong response signal from the satellite.

Section 2 will describe the new concept including background information on VCSEL / Photodetector Arrays and will present preliminary computer simulations using the optics code, OpticStudio, from Zemax, LLC<sup>6</sup>. These simulations use the capabilities in the Physical Optics Propagation option in the code to model the laser source and diffraction effects from wave optics. These capabilities make it possible to model laser beam propagation over long space communication distances. Section 3 will discuss the application of this system to LLO. Section 4 will present a brief summary of these developments.

## 2 NEW CONCEPT FOR LASER BEAM POINTING

### 2.1 Technical Approach

As Fig. 1 shows, an incoming laser beam (green or blue, with rightward arrows), transmitted from a ground terminal, enters the lens system, which directs it to an element of the pixel array (gray rectangle). Each element, or pixel, consists of a VCSEL component/Photodetector pair. The photodetector detects the possibly weak signal beam, and the VCSEL component returns a strong modulated beam to the lens system (green or blue, with leftward arrows), which sends it to the ground terminal. As the incoming beam changes direction, e.g., from the blue to the green incoming direction, this change is detected by the adjacent photodetector, and the laser paired with that photodetector is turned on to keep the outgoing laser beam on target. The laser beams overlap so that the returning beam continues to point at the ground terminal. The VCSEL component may consist of a single VCSEL or a cluster of VCSELs. Alternatively, a VCSEL component from a different element could send the returning beam along a slightly different outgoing path to account for “pointing ahead”. The laser beams are incoherent to avoid interference effects. With incoherent outgoing beams from adjacent lasers, they can overlap so that the returning beam continues to point at the ground terminal without self-interference.

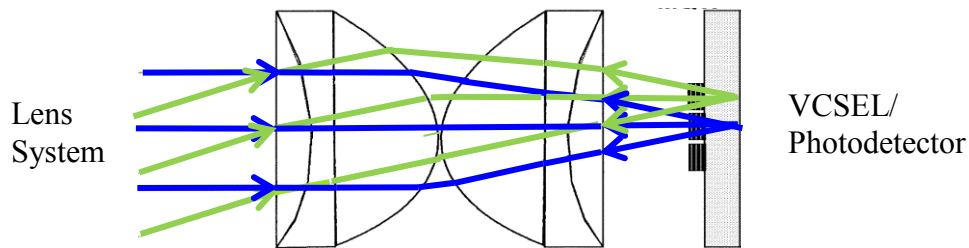


Fig. 1: Space Optical Communications using a Lens System with a Vertical Cavity Surface Emitting Laser (VCSEL)/ Photodetector Array

The outgoing beam may be much stronger than the incoming beam, depending only on the power of the VCSEL. For various levels of outgoing power, the VCSEL component may consist of a single VCSEL or a cluster of VCSELs. The use of a cluster of VCSELs rather than a larger aperture VCSEL maintains the restriction to a single-mode laser beam. The VCSEL cluster will emit several incoherent beams that are all single-mode. This restriction is desirable to facilitate the detection of the beam at the receiver by avoiding multi-modes in the beam. The output power of a cluster of VCSELs will be slightly less than the sum of the outputs of the individual VCSELs due to thermal crosstalk effects, but these effects will not prevent VCSEL clusters from providing the desired output power.

## 2.2 VCSEL/ Photodetector Array

Figure 2 shows a candidate VCSEL/ Photodetector Array. In this array the pitch, (i.e., the distance between elements), is the same for the VCSEL clusters and the photodetectors. Also, this packing pattern makes the distance between adjacent elements equal.

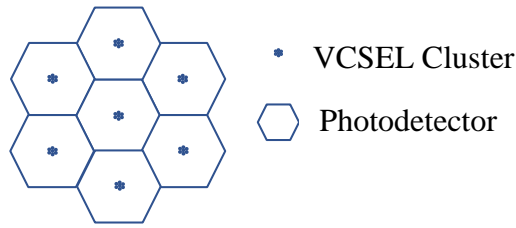
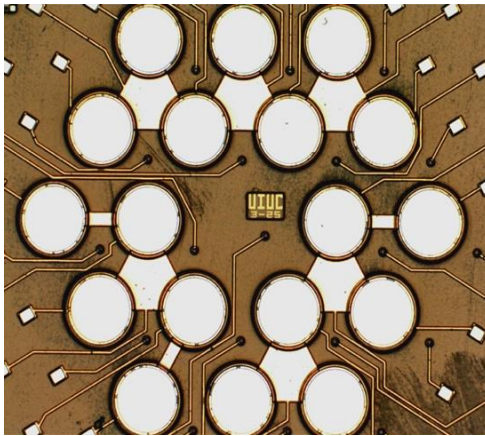
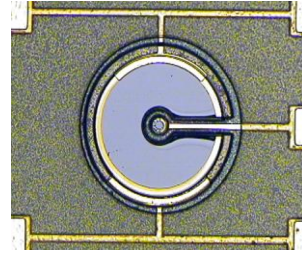


Fig. 2: Candidate VCSEL/ Photodetector Array

Figure 3 shows a fabricated<sup>7</sup> VCSEL/ Photodetector Array<sup>7</sup> and a fabricated VCSEL/Photodetector pair. The Photodetectors are p-type/intrinsic/n-type (PIN) detectors.



3a)



3b)

Figure 3:

- a) Top-view of a 37-element VCSEL / PIN detector array. VCSELs are small black dots and photodetectors are large white circles,
- b) Top-view of a VCSEL /Photodetector pair

## 3 LLO APPLICATION

### 3.1 Example of Telescope Lens System

Preliminary analysis<sup>2</sup> indicates that this VCSEL / PIN detector array system can be incorporated into a small telescope to make the steering finer and consequently be applicable to transmissions between CubeSats in low lunar orbit (LLO) and ground terminals. Figure 4 shows a lens design where a small telescope is placed in front of the lens/laser array system to reduce the angle  $\beta$  of the beam propagation emitted from the lens/laser array system to the smaller angle  $\alpha$  of the beam propagation emitted from the objective lens of the telescope. Without the telescope, the spots from two adjacent laser beams from a satellite in LEO may not overlap on the Moon, so there would be a loss of coverage of the beam at the ground terminal as the direction from the lens system to the ground terminal changed. The telescope design details depend on the design parameters of the lens/laser array system, the distance to the ground terminal, the size of the beam spot size, and the sensitivity of the ground receiver. The magnification of the telescope  $M = f_o/f_e$ , where  $f_o$  is the focal

length of the objective lens and  $f_e$  is the focal length of the eyepiece lens. Also,  $M = \beta/\alpha$ , so that the angle of the outgoing beam is reduced for finer aiming.

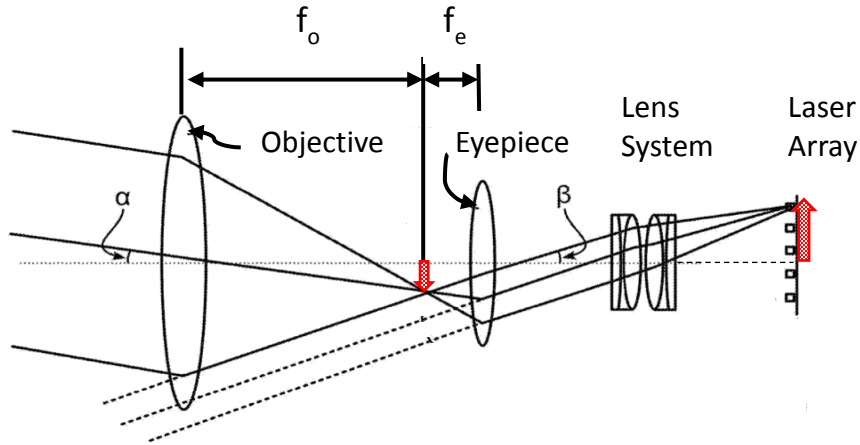


Figure 4: A telescope and lens/laser array system.

An application will be made to show how this new pointing system can be used to augment a laser pointing system on a CubeSat in LLO that uses star trackers for body pointing. The new pointing system would provide a fine-pointing capability to the CubeSat body pointing system. With the resulting more accurate pointing, the power requirement would be substantially reduced and the resulting thermal load also reduced, thereby mitigating the current thermal load challenge.

### 3.2 CubeSat that uses body pointing of laser beams without fine pointing

Figure 5 shows the irradiance and phase of the wave front at 100 km of propagation, a LLO distance, for a laser beam with a divergence of  $0.46^\circ$ , without using fine pointing. The laser beam wavelength is 1064 nm, the laser output power is 2 W and the peak irradiance of the beam at the image plane is  $7.11 \times 10^{-13} \text{ W}/(\text{mm})^2$ . The irradiance has a Gaussian profile, and the phase is essentially flat, so that this beam is diffraction limited. The units for the distances in Fig. 5 are in mm and the spot size is about 1600 m.

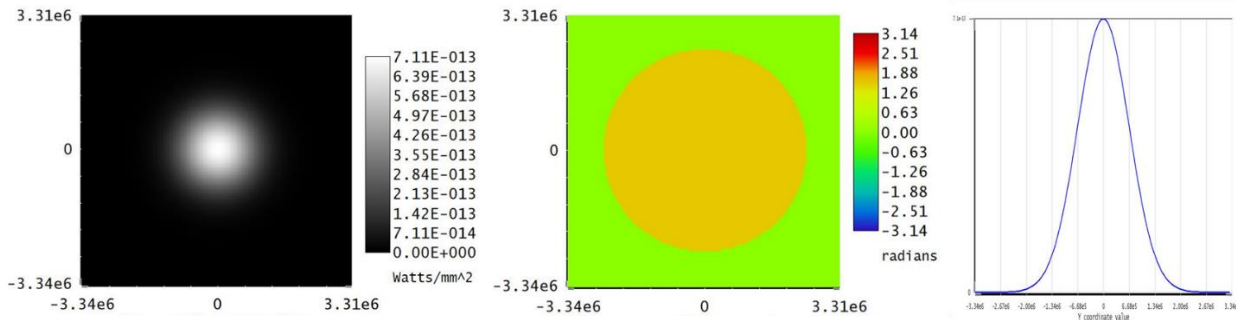


Figure 5: a) irradiance, b) phase, c) Y-coordinate cross-section of irradiance

### 3.3 CubeSat that uses body pointing of laser beams with fine pointing

A new lens design is shown in Fig. 6. It consists of three lens systems, each with four lens elements. The four lens elements consist of two doublets with the left doublet's elements in reverse order from that of the right doublet. The lens systems are examples of a modern version of the symmetrical Plössl design, which is used as an eyepiece for telescopes.<sup>8</sup> The lens system C was the starting design for the new system. The lens system B is a reduction of the lens system C by

a factor of sixteen; together they form a miniature telescope with a magnification factor of sixteen. The lens system A converts a diverging beam from the laser array plane into a collimated beam for entry into the telescope system. Lens system A retains the radii of the lens system C and its focal length to minimize the angle of a laser beam from a laser in the array to the vertex of the first surface of lens system A. In addition, there are micro-lenses<sup>9</sup> (not shown) in front of each laser in the array to narrow the emerging beam and point it to the center of the lens systems stop, which is located between lens system A and lens system B. The focal plane is where lens system B focuses the beam. The distances from the last surface of lens system B to the focal plane and from the focal plane to the first surface of lens system C indicate approximately  $f_e$ , the focal length of the eyepiece lens and  $f_o$ , the focal length of the objective lens respectively. The telescope's effect is to reduce the divergence of the beam and broaden the beam, both by the magnification of the telescope  $M = f_o/f_e$ , a factor of sixteen.

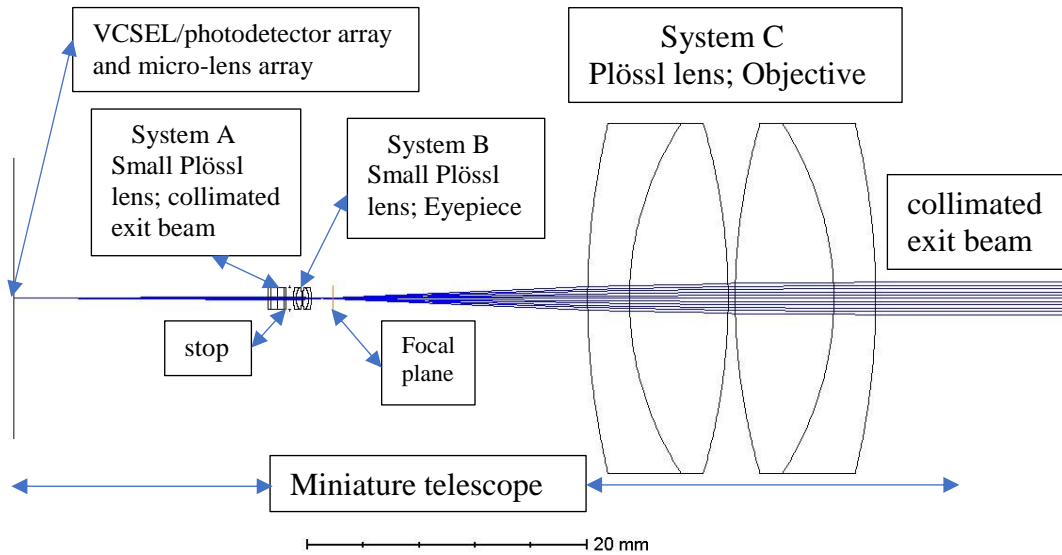


Figure 6: New lens system using Plössl lenses

A Plössl lens is used here for simulating the beam propagation through the new lens system as a proof-of-concept demonstration. The length of the entire system is 47 mm, from the location of the VCSEL/photodetector array on the left (vertical line) to the last lens surface on the right. The diameter of the lenses on the right is 25 mm, which should be large enough to collect enough light for the photodetectors to detect the incoming beam. However, it may be possible to design a lens system that is smaller. The Plössl lens was not designed for space communications, and the beam diameter at the last lens surface is 1.5 mm FWHM. (The beam shown in Fig. 6 is for illustrative purposes; the actual beam from the calculations is narrower.)

Figure 7 shows the irradiance and phase of the wave front at 100 km for the laser beam from the new lens system shown in Fig. 6. The beam has a divergence of  $0.057^\circ$  FWHM, and the diameter of the spot size at the image plane is about 200 m. The output power from the laser cluster is 30 mW, and the peak irradiance of the beam is  $7.08 \times 10^{-13} \text{ W}/(\text{mm})^2$ , which is almost the same as the  $7.11 \times 10^{-13} \text{ W}/(\text{mm})^2$  for the 2 W beam with a divergence of  $0.14^\circ$  FWHM. The irradiance has a Gaussian profile, and the phase is essentially flat, so that this beam is diffraction limited. The units for the distances are in mm.

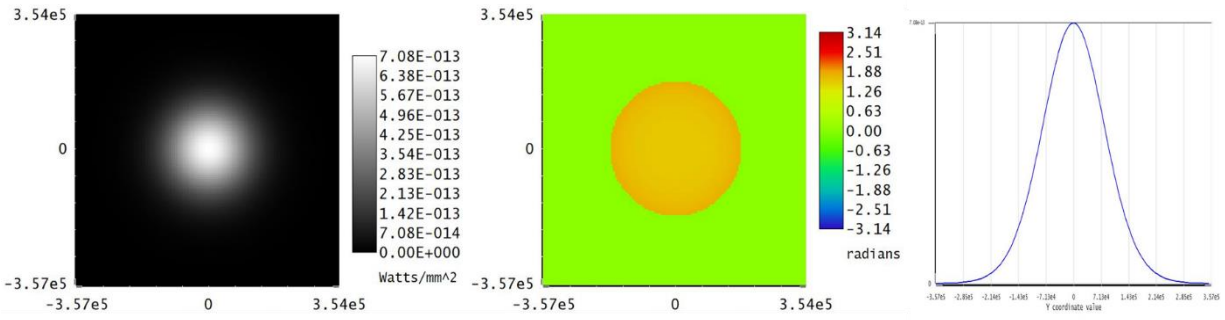


Figure 7: a) irradiance, b) phase, c) Y-coordinate cross- section of irradiance

Next the results of the simulation of two and then three incoherent beams simultaneously propagating will be shown. The resulting combined beam will form a plateau at the peak, so that changes in direction of that beam with respect to the receiver will not affect the intensity of the beam at the receiver, as long as the receiver is within the plateau area. This insensitivity is not possible if just one beam is transmitted.

The results in Fig7 are for a VCSEL or VCSEL cluster, as shown in Fig. 2, in the array at the focal plane of lens System A whose center is located on the axis of the lens system, namely  $x = y = 0$ . Now results will be shown for  $x = 0, y = 83 \mu\text{m}$ . The pitch between the two lasers or laser clusters is also  $83 \mu\text{m}$ .

Figure 8 shows the irradiance and phase of the wave front at 100 km for the laser beam from the laser located at  $x = 0, y = 83 \mu\text{m}$ . Again, the output power from the laser cluster is 30 mW and now the peak irradiance of the beam is  $6.99 \times 10^{-13} \text{ W}/(\text{mm})^2$ . As for the beam from the laser located at  $x = 0, y = 0 \mu\text{m}$ , the irradiance has a Gaussian profile, and the phase is essentially flat, so that this beam is diffraction limited. The center of the beam is about 200 m up from the center of the beam in Fig.7.

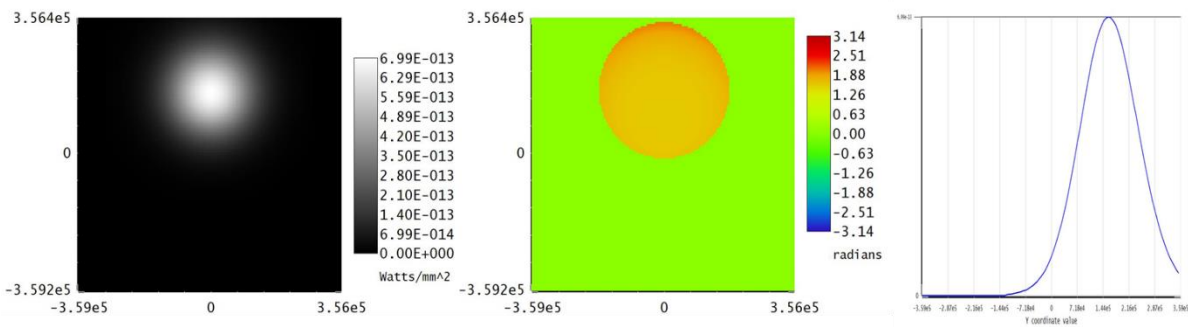
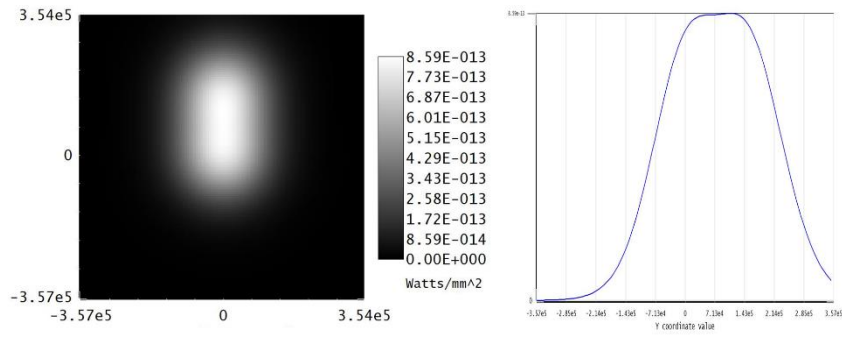


Figure 8: a) irradiance, b) phase, c) Y-coordinate cross- section of irradiance

Figure 9 shows the resulting beam when the two lasers are turned on together; the beam is the combination of the two incoherent beams shown in Figs. 7 and 8. There is a plateau region formed by the two laser beams. There is no phase plot since the beams are incoherent. The output power from the two laser clusters is 60 mW.



a) irradiance,

b) Y-coordinate cross-section of irradiance.

Figure 9: Two combined beams

In Fig. 10, results are shown for  $x = 72$ ,  $y = 42 \mu\text{m}$ . The pitch between the three lasers or laser clusters is  $87 \mu\text{m}$ . Again, the output power from the laser cluster is  $30 \text{ mW}$  and again the peak irradiance of the beam is  $6.99 \times 10^{-13} \text{ W}/(\text{mm})^2$ . As for the first two beams, the irradiance for the third beam has a Gaussian profile, and the phase is essentially flat, so that this beam is diffraction limited. The center of the beam is equidistant from the centers of the beams in Figs. 7 and 8.

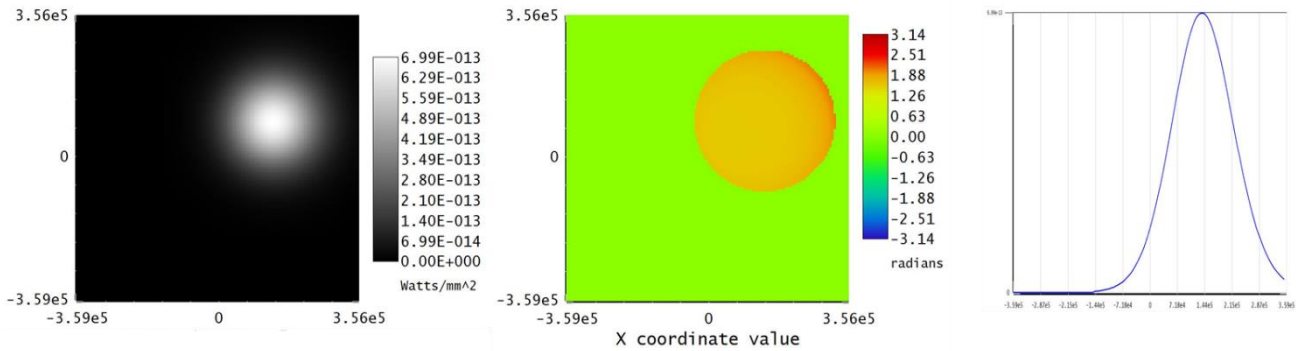


Figure 10: a) irradiance,  
X-coordinate cross-section of irradiance

b) phase, c)

Figure 11 shows the resulting beam when the three lasers are turned on together; the beam is the combination of the three incoherent beams shown in Figs. 7, 8 and 10. They illuminate a triangular area. There is no phase plot since the beams are incoherent. In Fig. 20 b), the x-coordinate cross-section is taken at a  $y$  value halfway between the centers of the two beams in Fig. 9, at which  $y = 100 \text{ m}$  in the image plane. The output power from the three laser clusters is  $90 \text{ mW}$ .

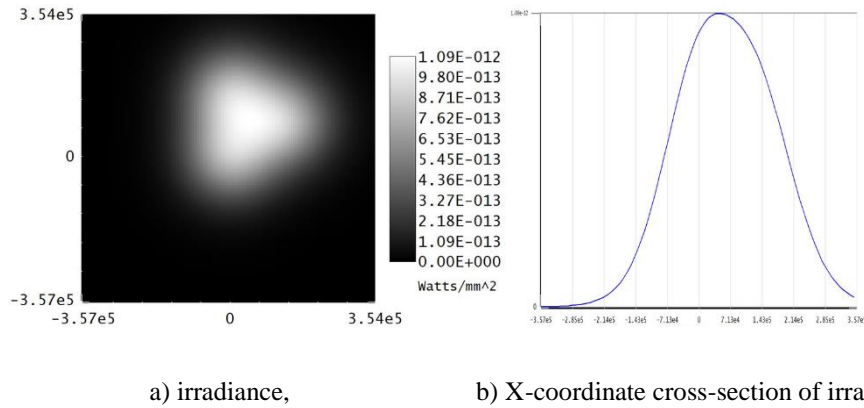


Figure 11: Three combined beams

### 3.4 Fine Pointing Capability

Now a comparison will be made of the laser beam from one laser with an output power of 2 W, as shown in Sec. 3.2 and of the laser beams in Sec.3.3. The spot size of the laser beam shown in Sec. 3.2 is 1600 m in diameter FWHM and the spot size of one beam in Sec. 3.3 is 200 m. As shown in Fig. 11, a distance of 200 m between the centers of the spots assures that laser beams overlap so that the returning beam continues to point at the ground terminal as the direction of the satellite changes. By increasing the number of PIN elements in Fig. 2 but keeping the pattern the same, so that there are 64 PIN elements and 42 VCSEL clusters,<sup>7,9</sup> the area covered by all the beams would cover the area covered by the beam shown in Fig. 5. Now the procedure explained in Sec. 2.1 could be applied. When a PIN detects an incoming signal beam, the VCSEL cluster in the VCSEL /Photodetector pair would be turned on. A VCSEL cluster could consist of seven VCSELs, each with a power of about 4 mW. This fine pointing capability would augment the body pointing system of the CubeSat, the power requirement for the laser beam would be reduced, and the resulting thermal load would be reduced. The fine pointing device is static and would avoid the need for of an optical gimbal or any internal beam steering hardware with moving parts.

### 3.5 Optical Multiple Access (OMA)

Simultaneous optical multiple access (OMA) is possible from different transceivers within the area covered by the laser array. Since laser beams from different sources come in at different angles and then get mapped to different photodetectors; the lasers in those VCSEL/Photodetector pairs can simultaneously send laser beams back to the different sources.

## 4 SUMMARY

A new method has been described for optical data transmissions from CubeSats in LLO that use body pointing for laser beams. The new method uses laser arrays to provide fine pointing of the laser beams. It combines a lens system and a VCSEL/Photodetector Array, both mature technologies, in a novel way. The concept is described and some features of the array are explained. With fine pointing, the simulations showed that the spot size on the moon could be reduced by a factor of eight with a reduction in laser output power by a factor of sixty-four, thereby mitigating the thermal load on the CubeSats.



